

First observation of excited structures in neutron deficient, odd-mass Pt, Au and Hg nuclei

F.G. Kondev^a, M.P. Carpenter^a, R.V.F. Janssens^a, K. Abu Saleem^{a,b}, I. Ahmad^a, M. Alcorta^a, H. Amro^{a,c}, J. Caggiano^a, J.A. Cizewski^d, M. Danchev^e, C.N. Davids^a, D.J. Hartley^e, A. Heinz^a, B. Herskind^f, R.A. Kaye^{a,*}, T.L. Khoo^a, T. Lauritsen^a, C.J. Lister^a, W.C. Ma^c, G.L. Poli^a, J. Ressler^{a,g}, W. Reviol^{e,†}, L.L. Riedinger^e, D. Seweryniak^a, S. Siem^{a,‡}, M.B. Smith^d, A.A. Sonzogni^a, P.G. Varmette^c, and I. Wiedenhöver^{a,§}

^aPhysics Division, Argonne National Laboratory, Argonne, IL 60439, USA

^bDepartment of Physics, Illinois Institute of Technology, Chicago, IL 60616, USA

^cDepartment of Physics, Mississippi State University, Starkville, MS 39762, USA

^dDepartment of Physics and Astronomy, Rutgers University, New Brunswick, NJ 08903, USA

^eDepartment of Physics and Astronomy, University of Tennessee, Knoxville, TN 37996, USA

^fThe Niels Bohr Institute, Riso 4000, Roskilde, Denmark

^gDepartment of Chemistry, University of Maryland, College Park, MD 20742, USA

Excited structures in neutron-deficient Pt, Au and Hg isotopes have been investigated for the first time using the Gammasphere spectrometer in conjunction with the recoil-decay tagging technique. Illustrative examples are presented and discussed in the context of shape coexistence in the vicinity of the proton-drip line.

1. INTRODUCTION

Coexistence between different shapes in a single nucleus is a general phenomenon of nuclei located near shell gaps. This phenomenon is usually associated with the interplay between the occupation of specific intruder orbitals and the stabilizing role played by shell closures. Experimental investigations of the development of shape coexistence through

*Present address: Department of Chemistry and Physics, Purdue University Calumet, Hammond, IN 46232, USA

†Present address: Department of Chemistry, Washington University, St. Louis, MO 63130, USA

‡Present address: Department of Physics, University of Oslo, N-0316 Oslo, Norway

§Present address: National Superconducting Cyclotron Laboratory, Michigan State University, East Lansing, MI 48824, USA

and beyond mid-shell, and of the interactions between coexisting configurations, play an important role in understanding the structure of nuclei at the extremes in N/Z ratio, excitation energy and angular momentum. They also provide opportunities to test the ability of various theoretical models to predict single-particle states near the proton-drip line and to describe their effect on the onset of new shell closures.

Nuclei around the $Z = 82$ shell gap provide some of the best examples of shape coexistence known so far. For instance, the ^{186}Pb isotope is observed to form *three* minima at low spin [1], associated with spherical, oblate and prolate shapes. While the former is attributed to the proximity of the $Z = 82$ closure, the prolate and oblate shapes are associated with particle-hole ($p-h$) excitations into proton $h_{9/2}$, $f_{7/2}$ and $i_{13/2}$ low- Ω (prolate) and high- Ω (oblate) intruder orbitals [2]. Furthermore, calculations by Bengtsson and Nazarewicz [3], and Nazarewicz [4], as well as the systematic studies of near mid-shell nuclei by Dracoulis [5], have stressed the role of more complicated multi-particle-hole excitations. There is also an additional increase in shell stability for specific configurations involved in the prolate and oblate minima due to the presence of sub-shell gaps at $N = 98$ ($\beta_2 \sim 0.25$) and $Z = 80$ ($\beta_2 \sim -0.15$). At low-spin, however, the neutron-deficient, even-even Hg ($Z = 80$) isotopes show a coexistence between only *two* shapes, i.e. a weakly deformed *oblate* ground state and a more deformed excited *prolate* band. Similar trends have been established in the mid-shell Pt isotopes, albeit the situation is reversed in the sense that the prolate structures are lower in energy. Recent studies of $^{168,170}\text{Pt}$ [6] and $^{176,178}\text{Hg}$ [7–9] have revealed that in nuclei near the proton-drip line the excitation energy of the prolate minimum rises with respect to the oblate one to the point where there is no longer any clear evidence for its presence at low spin.

In order to elucidate the role played by the valence orbitals on the structure of the even-even core, it is important to investigate the neighboring odd-mass nuclei. Furthermore, the odd nucleon itself can have a significant impact on the nuclear shape by driving the deformation itself, or by blocking some component of the microscopic core configuration. Knowledge about shape evolution near the proton-drip line is rather scarce. This is partially due to the paucity of experimental data. It is clearly of interest to pursue the exploration of the structure of the odd-mass Pt, Au and Hg isotopes towards lower neutron number in order to test various model predictions in the vicinity of the proton-drip line.

In this paper we report on the first observation of excited states in many neutron-deficient, odd-mass Pt, Au and Hg nuclei. The high sensitivity in the present measurements is achieved by using the prompt γ -ray coincidence technique following mass selection in conjunction with the recoil-decay tagging technique [10]. Further suppression of fission and charged particle emission was achieved by employing fusion reactions of symmetric nuclei, which are characterized by large and negative Q values, at energies near the barrier.

2. EXPERIMENTAL PROCEDURE

Excited states in neutron-deficient Pt, Au and Hg nuclei were populated using symmetric, fusion reactions with beams delivered by the ATLAS superconducting linear accelerator at Argonne National Laboratory. A list of the reactions used, the characteristics of the targets and the beam energies is given in Table I. Prompt γ rays were detected

Table 1

Reactions, beam energies and target compositions.

Reaction	Beam energy (MeV)	Target	Abundance (%)	Thickness ($\mu\text{g}/\text{cm}^2$)
$^{90}\text{Zr}+^{90}\text{Zr}$	369, 380	^{90}Zr	97.65	550
$^{90}\text{Zr}+^{91}\text{Zr}$	380	^{91}Zr	89.20	560
$^{84}\text{Sr}+^{92}\text{Mo}$	390, 395	^{92}Mo	98.27	770
$^{84}\text{Sr}+^{94}\text{Mo}$	380, 385	^{94}Mo	91.59	660
$^{84}\text{Sr}+^{96}\text{Mo}$	380	^{96}Mo	96.76	700

with the Gammasphere array [11] consisting, for these experiments, of 101 large volume escape-suppressed Ge detectors. The recoiling products passed through the Argonne Fragment Mass Analyzer (FMA) [12] and were dispersed according to their mass-to-charge (m/q) ratio. A $5 \mu\text{g}/\text{cm}^2$ thick carbon foil was located ~ 8 cm behind the target to reset the charge state distribution of the recoiling nuclei. A position-sensitive parallel grid avalanche counter (PGAC), located at the focal plane, provided the m/q information as well as time of arrival and energy-loss signals of the evaporation residues. The recoiling nuclei were subsequently implanted into a 40×40 strips ($40 \text{ mm} \times 40 \text{ mm}$, $\sim 60 \mu\text{m}$ thick), double-sided silicon strip detector (DSSD) located 40 cm behind the PGAC. This DSSD was used not only to detect the implantation of a residue and to determine its time of arrival with respect to the prompt γ -ray flash detected by Gammasphere, but also to measure its subsequent α decay(s). For this purpose, the DSSD events were time-stamped using a 47-bit, 1 MHz clock. The high pixel segmentation of the DSSD provided effective spatial and time correlations between the implants and the subsequent α decays.

Specific details regarding the experiments and the data reduction are given in Refs. [13, 14]. It is worth noting that during the experiments with a ^{84}Sr beam, an array consisting of four Gammasphere-type HpGe detectors and a single LEPS detector surrounded the DSSD. Time-correlated $\alpha - \gamma$ coincidence measurements were carried out in order to elucidate the α decay to excited levels in the daughter nucleus and, hence, to provide unambiguous spin and parity assignments.

3. RESULTS AND DISCUSSION

The present study provided gamma-ray spectroscopy information about more than 20 neutron-deficient Pt, Au and Hg isotopes: a summary is shown in Fig. 1. It is worth noting that 11 of these were investigated for the first time in the present work and that we added significantly to the structure of previously studied nuclei in the region. Illustrative examples focussing on the role played by specific neutron and proton configurations are discussed below.

3.1. Spectroscopy of odd-N $^{173,175}\text{Pt}$ ($Z = 78$) and ^{179}Hg ($Z = 80$) isotopes

Excited states in ^{179}Hg were populated in the $1n$ channel of the symmetric $^{90}\text{Zr}+^{90}\text{Zr}$ reaction. The striking feature of the level scheme is the competition between structures associated with three different minima: weakly prolate (triaxial), oblate and prolate. By

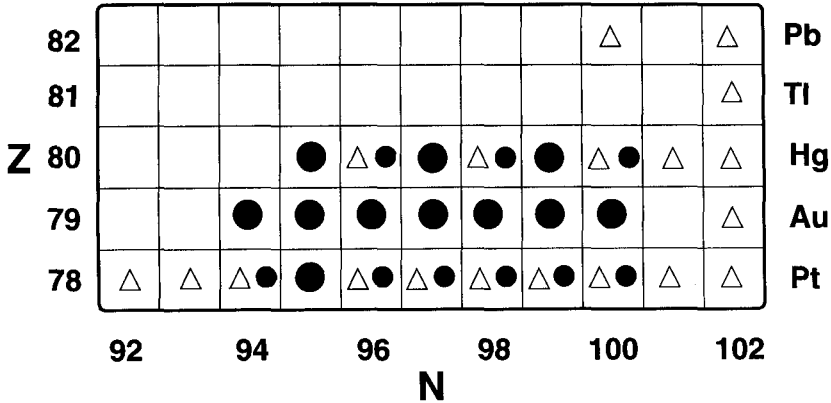


Figure 1. Summary of nuclei studied in the present work (filled circles) and nuclei known from previous investigations (open triangles).

combining the simplicity of the α -decay properties of ^{179}Hg and of its daughter (^{175}Pt), and grand-daughter (^{171}Os) nuclei with the complexity of the γ -ray spectroscopic information we have established the spin and parity of the ^{179}Hg ground state as $7/2^-$ and assigned it the mixed $f_{7/2}/h_{9/2}$ configuration which originates from a weakly prolate (triaxial) shape. This observation is supported by complementary total Routhian surface (TRS) calculations which predict $\beta_2=0.112$ and $\gamma\sim 37^\circ$ for the above configuration. Three prolate collective bands were observed to compete for favored yrast status at higher excitation energies. These were assigned the $5/2^-$ [512], $1/2^-$ [521] and $7/2^+$ [633] Nilsson configurations on the basis of the measured in-band properties such as branching ratios and alignments, as well as on considerations about which orbitals are expected near the neutron Fermi surface. Similarities with known structures in neighboring odd-mass Hg and Pt nuclei were also helpful. A high-spin $13/2^+$ isomer, analogous to those seen in the heavier Hg isotopes [15–17], has also been observed and assigned the oblate $13/2^+$ [606] configuration. The existence of multiple shapes is a unique feature of ^{179}Hg when compared to the heavier odd-mass $^{181,183,185}\text{Hg}$ isotopes [15–17]. We also found evidence for competing triaxial and prolate structures in ^{175}Pt ($N = 97$), whose properties match closely those of ^{179}Hg , with the exception that the oblate minimum rises significantly in energy at $Z = 78$ and has not been observed experimentally. We observed for the first time excited bands in ^{175}Pt , most likely of negative parity, feeding directly the $7/2^-$ ground state. In addition, we extended the previously known $\nu i_{13/2}$ yrast band [18] in spin and we placed the $13/2^+$ bandhead at 171 keV above the ground state. With two neutrons less, however, the yrast structure of ^{173}Pt ($N = 95$) is dominated by a single $\Delta I=2$ band which is assigned a low- Ω $i_{13/2}$ configuration. Its deformation is lower than that found for the corresponding band in ^{175}Pt , as evident from the systematics of transition energies shown in Fig. 2a. The decline in deformation below mid-shell occurs in a rather smooth way as the neutron number decreases. This can be partially attributed to the stepwise emptying of the low- Ω $i_{13/2}$ neutron intruder orbitals.

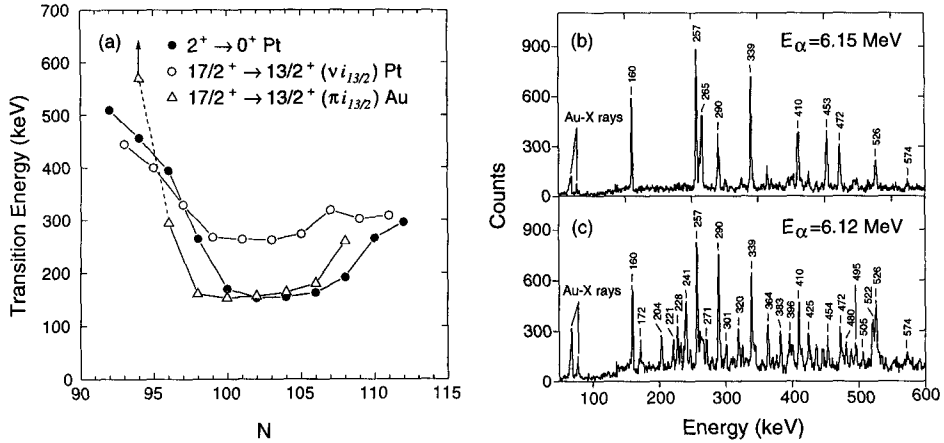


Figure 2. (a) Systematics of transition energies for selected Pt and Au isotopes. Gamma-ray spectra correlated with the $E_\alpha = 6.15$ MeV (b) and $E_\alpha = 6.12$ MeV (c) lines of ^{177}Au .

3.2. Spectroscopy of odd- Z ($Z = 79$) $^{173,175,177}\text{Au}$ isotopes

The investigations of neutron-deficient gold isotopes add information on the relative importance of various proton configurations in defining the deformation. Collective structures arising from the low- Ω $h_{9/2}$, $f_{7/2}$ and $i_{13/2}$ proton orbitals have recently been observed in $^{179,181,183}\text{Au}$ [19]. Here we have focussed on the isotopes ^{173}Au ($N = 94$), ^{175}Au ($N = 96$) and ^{177}Au ($N = 98$). The main observed features can be summarized as follow: (a) A high-spin $I^\pi = 11/2^-$ isomer arising from the $11/2^- [505] (h_{11/2})$ configuration has been observed in all three isotopes. A low-spin isomer has been also established, but only in ^{173}Au and ^{177}Au . Figures 2(b) and 2(c) show γ -ray spectra correlated with the two isomeric states in ^{177}Au and marked differences can be seen.

(b) While the yrast structure of ^{175}Au and ^{177}Au is formed by a prolate band originating from the $i_{13/2}$ proton configuration, no sign of collectivity is observed in ^{173}Au .

(c) The excitation energy of the prolate minimum is found to rise rapidly in energy as the neutron number decreases, thus suggesting a decline in deformation.

(d) There is evidence for structures originating from three minima: spherical, oblate and prolate, in ^{175}Au .

The deformation trend for the $i_{13/2}$ proton bands in odd-mass Au isotopes can be qualitatively deduced from Fig. 2(a). While their behavior follows that of the core for $N > 100$, there is an abrupt loss of collectivity below $N = 96$. Furthermore, the observation of well-deformed, prolate bands in ^{175}Au and ^{177}Au suggests that the blocking of the low- Ω $i_{13/2}$ proton orbital does not preclude the development of the prolate minimum. This would support the view [3–5] that more complicated multi-particle-hole configurations are involved in the structure of the prolate minimum.

ACKNOWLEDGMENT

The authors wish to thank the staff of the ATLAS accelerator facility and the Physics Support Group for their assistance in various phases of the experiment. We are grateful to J. P. Greene for the preparation of the targets. The software support by D. C. Radford and H. Q. Jin is greatly appreciated. Discussions with M. A. Riley and G. D. Dracoulis are gratefully acknowledged. This work is supported by the U.S. Department of Energy, Nuclear Physics Division, under Contracts No. W-31-109-ENG-38, DE-FG02-96ER40983 and DE-FG02-95ER40939.

REFERENCES

1. A. N. Andreyev *et al.*, Nature 405 (2000) 430 and contribution to these proceedings.
2. J. L. Wood, K. Heyde, W. Nazarewicz, M. Huyse, and P. Van Duppen, Phys. Rep. 215 (1992) 103 and references therein; K. Heyde, P. Van Isacker, M. Waroquier, J. L. Wood, and R. A. Meyer, Phys. Rep. 102 (1983) 293 and references therein.
3. R. Bengtsson and W. Nazarewicz, Z. Phys. A334 (1989) 269.
4. W. Nazarewicz, Phys. Lett. B305 (1993) 195.
5. G. D. Dracoulis, Phys. Rev. C49 (1994) 3324.
6. S. King *et al.*, Phys. Lett. B443 (1998) 82.
7. M. P. Carpenter *et al.*, Phys. Rev. Lett. 78 (1997) 3650.
8. M. Muikku *et al.*, Phys. Rev. C58 (1998) R3033.
9. F. G. Kondev *et al.*, Phys. Rev. C61 (2000) 011303(R).
10. E. S. Paul *et al.*, Phys. Rev. C 51 (1995) 71.; R. S. Simon *et al.*, Z. Phys. A325 (1986) 197.
11. I. Y. Lee, Nucl. Phys. A520 (1990) 641c.
12. C. N. Davids, B. B. Back, K. Bindra, D. J. Henderson, W. Kutschera, T. Lauritsen, Y. Nagame, P. Sugathan, A. V. Ramayya, and W. B. Walters, Nucl. Instrum. Methods Phys. Res. B70 (1992) 358.
13. F. G. Kondev *et al.*, Phys. Rev. C61 (2000) 044323.
14. F. G. Kondev *et al.*, Phys. Rev. C62 (2000) 044305.
15. P. G. Varmette *et al.*, Phys. Lett. B410 (1997) 103.
16. G. J. Lane, G. D. Dracoulis, A. P. Byrne, S. S. Andersen, P. M. Davidson, B. Fabricius, T. Kibédi, A. E. Stuchbery and A. M. Baxter, Nucl. Phys. A589 (1995) 129.
17. F. Hannachi, G. Bastin, M. G. Porquet, J. P. Thibaud, C. Bourgeois, L. Hildingsson, N. Perrin, H. Sergolle, F. A. Beck and J. C. Merdinger, Z. Phys. A330 (1988) 15.
18. B. Cederwall *et al.*, Z. Phys. A337 (1990) 283.
19. W. F. Mueller *et al.*, Phys. Rev. C59 (1999) 2009.; W. F. Mueller *et al.*, to be published.